Journal of Nanomaterials and Applications

Reconstructing Spin Theory: A Constrained Medium Framework for Gravitation and Electromagnetism

Dung Nguyen Trong[1,*], Ştefan Ţălu [2]

[1] Faculty of Applied Sciences, University of Transport Technology, 54 Trieu Khuc, 100000, Hanoi, Vietnam.

[2] The Directorate of Research, Development and Innovation Management (DMCDI), Technical University of Cluj-Napoca, 15 Constantin Daicoviciu St., Cluj-Napoca, 400020, Cluj county, Romania.

Review info

Type of articles:
Review article

Corresponding author*:
Dung Nguyen Trong:
dungnt78@utt.edu.vn

Received: 07 October 2026
Revised: 14 November 2026
Accepted: 15 November 2026
Published:28 November 2026

Abstract: Medium formulations of relativistic physics offer a concrete mechanistic ontology while remaining empirically consistent with standard theories. We present the Extended Spin-Medium Theory (ESMT), a constrained mathematical reconstruction of the heuristic "Spin Theory." After eliminating algebraic inconsistencies and empirically refuted claims from the original proposal, ESMT establishes eight axioms defined on flat Euclidean slices with absolute time, defining medium spin as local vorticity $\Omega = \frac{1}{2}\nabla \times v$. ESMT (i) unifies kinematic and gravitational time dilation into a single clock-rate relation, matching GR consistency checks including the $+38.576\ \mu s/day$ GPS offset; (ii) identifies medium spin with Lense–Thirring precession in the weak-field limit; (iii) maps Maxwell's equations to MacCullagh rotational elasticity; and (iv) formulates flat cosmology as a center-free Hubble flow. Beyond standard GR equivalences, ESMT introduces four falsifiable predictions, including a Lorentz-violation signal template locked to the cosmic microwave background (CMB) dipole.

Keywords: analogue gravity; emergent Lorentz invariance; gravitomagnetism; MacCullagh aether; Painlevé–Gullstrand coordinates; preferred frame; river model of gravity; tests of general relativity.

1. Introduction

1.1. Background and motivation

General relativity (GR) and quantum field theory have passed every test within their domains of validity [1,2]. Their mutual incompatibility at the Planck scale, the nature of dark energy and dark matter, and the origin of spacetime structure itself nevertheless remain open. A substantial line of research holds that spacetime and gauge fields may not be fundamental but may instead emerge from a microscopic medium,

in the same way that the wave equation of sound emerges from a fluid [3–6]. In such models Lorentz invariance is an approximate low-energy symmetry, and a microscopic preferred frame exists that is not directly observable [7,8].

The "Spin Theory" [9] is an independent programme, motivated by classical physical intuition, that points in the same direction: absolute Euclidean space, absolute time, a plenum of elements endowed with spin, and interactions understood as exchanges of spin. What the original formulation lacks is not physical intuition but mathematical structure: its laws are stated verbally or through algebraic manipulations that do not survive scrutiny, so that the theory yields no quantitative predictions. The question addressed here is therefore methodological as much as physical: how much of the ontology of such a programme can be retained once every law is required to be formally consistent, dimensionally correct and quantitatively compatible with precision data?

1.2 Approach

We adopt a protocol of constrained reconstruction. The ontological assumptions of the source theory are retained wherever possible, and each assumption or law is tested against three criteria: (C1) formal consistency; (C2) compatibility with data at the measured precision; and (C3) the existence of a mathematical structure that produces numbers. Assumptions satisfying all three are kept; those violating one or more are replaced by the closest structure, in spirit, that satisfies them; those that cannot be rescued are discarded with a quantitative reason. Every structure introduced beyond standard physics must entail at least one testable consequence, in Popper's sense.

Conventions. We use SI units and the metric signature $(-,+,+,+)$. Bold symbols denote Euclidean three-vectors, an overdot denotes a derivative with respect to the absolute time t (except in Appendix C.2, where it denotes $d/d\tau$), and $\hat{\mathbf{r}}=\mathbf{r}/r$.

1.3 Contributions

The contributions of this paper are as follows.

A systematic audit of the source theory locating its formal errors and empirical conflicts, including a corrected quantitative exclusion of its Le Sage-type gravitational mechanism (Section 3 and Appendix A).

An eight-axiom formulation of ESMT in which "spin" is defined rigorously as the local angular velocity of the medium, $\Omega=\frac{1}{2}\nabla\times\mathbf{v}$ (Section 4).

A clock-rate theorem expressing all clock effects through a single quantity, the speed relative to the local medium, verified numerically against GPS, Pound–Rebka and Gravity Probe A (Sections 5 and 6).

An explicit weak-field identification of medium spin with gravitomagnetic (Lense–Thirring) precession (Section 5.4).

A representation of electromagnetism as rotational elasticity, and of flat cosmology as a Hubble flow, of the same medium (Sections 5.5 and 5.8).

A table of parameters, current bounds and falsifiable predictions, including a one-parameter signal template for preferred-frame searches (Section 7), together with an explicit statement of limitations (Section 8).

We emphasise at the outset that most of the mathematical structures used here are known individually. The contribution lies in their synthesis within a single ontology and in the demonstration that this ontology, once properly mathematised, is consistent with the data; Section 8.1 separates what is synthesis from what is genuinely new.

The paper is organised as follows. Section 2 reviews related work, and Section 3 audits the source theory.

Section 4 formulates the axioms of ESMT, and Section 5 derives its main results. Section 6 confronts the theory quantitatively with experiment, and Section 7 lists its parameters, current bounds and falsifiable predictions. Section 8 discusses novelty, the relation to general relativity and Einstein–aether theory, and the limitations of the approach; Section 9 outlines prospective applications, and Section 10 concludes. Detailed proofs and the numerical code are given in the appendices.

2 Related work

2.1 Classical medium programmes

The description of electromagnetic and optical phenomena as motions of a continuum has a history of almost two centuries. In 1839 MacCullagh proposed an aether whose elastic energy depends only on the rotation of its elements and not on compression or shear [10]. The model yields Fresnel's laws of reflection and refraction and was later recognised as exactly equivalent to Maxwell's equations in vacuum. In 1861–1862 Maxwell built a molecular-vortex model with idle-wheel particles, from which he obtained the displacement current and a wave speed equal to the speed of light [11]. In 1867 Kelvin proposed that atoms are stable vortex knots in the aether [12]. These models share the "spin is primitive" outlook of the Spin Theory; their enduring lesson is that a mechanical model is valuable only insofar as it generates equations.

2.2 Lorentzian aether and empirical indistinguishability

Lorentz's theory [13] assumes a stationary aether and absolute time and explains the null result of Michelson and Morley [14] through the dynamical contraction and slowing of moving bodies. It is empirically equivalent to special relativity [15]. Bell [16] and Brown [17] defended this dynamical approach as a legitimate, and physically illuminating, reading of relativity. Mansouri and Sexl [18] constructed a test theory with a preferred frame, and the Standard-Model Extension parametrises all possible Lorentz violations [2]; rotating-cavity experiments bound the anisotropy of the speed of light at the 10^{-17}–10^{-18} level [19,20].

2.3 Emergent gravity and acoustic geometry

Sakharov proposed that gravity is an induced "elasticity" of the vacuum [5]. Unruh showed that sound in a moving fluid propagates as a scalar field on an effective metric that can possess a horizon [21]. Visser systematised acoustic geometry [22], and Barceló, Liberati and Visser reviewed the whole field of analogue gravity [3]. Volovik showed that low-energy excitations of superfluid helium-3 behave as relativistic fermions, gauge fields and induced gravity [4]. Jacobson derived the Einstein equation as a thermodynamic equation of state [6]. Thermal Hawking radiation has been observed in an analogue black hole made from a Bose–Einstein condensate [23].

2.4 Modern dynamical aethers

Einstein–aether theory adds to GR a unit timelike vector field representing the four-velocity of a dynamical aether [7]; it is the modern framework closest in spirit to the Spin Theory. The binary neutron-star event GW170817 bounded the speed of gravitational waves to equal c within about 10^{-15} [24], eliminating much of the parameter space [8]. Post-Newtonian preferred-frame parameters α_1,α_2 are bounded by pulsar timing and lunar laser ranging [1,25,26].

2.5 The river model of gravity

In 1921–1922 Painlevé [27] and Gullstrand [28] independently found coordinates for the Schwarzschild solution in which spatial slices are flat and time is the proper time of observers falling freely from rest at

infinity. Hamilton and Lisle [29] showed that these coordinates permit an exact reading of a black hole as space flowing inward at the Newtonian escape velocity, with light moving at c relative to the local flow, and noted that in the rotating (Kerr) case the river acquires a twist. Doran found the corresponding form of the Kerr solution [30]. This structure is central to ESMT.

It is essential to distinguish ESMT from these established frameworks. In standard General Relativity, the Painlevé–Gullstrand (PG) metric and the River Model represent kinematic descriptions where the velocity field **v** is a gauge-dependent shift vector arising from a specific choice of spatial slicing. In contrast, ESMT promotes **v** to a physical continuum flow in a preferred absolute Euclidean space (E8). Unlike Einstein–aether theory [7], which introduces a dynamical timelike unit vector field into the action—inducing post-Newtonian preferred-frame parameters (α_1,α_2) and tensor-mode speed shifts tightly constrained by GW170817 [8, 24] minimal ESMT imposes no extra dynamical degrees of freedom in the low-energy gravity action. Instead, the preferred frame is fixed cosmologically by the Cosmic Microwave Background (CMB) rest frame. Consequently, ESMT functions as a non-dynamical background medium model that matches GR predictions identically in its domain of validity while isolating Lorentz-violating effects strictly to high-energy dispersion (E7) or CMB-aligned anisotropy (F1).

2.6 Particles as topological solitons and quantum hydrodynamics

Skyrme described baryons as topological solitons of the pion field [31]; Witten showed that the model is the large-N_c limit of quantum chromodynamics [32]; Finkelstein and Rubinstein proved that solitons can be quantised as fermions [33]. Faddeev and Niemi found stable knotted solitons, a realisation of Kelvin's vortex atoms [34]. Madelung showed that the Schrödinger equation is equivalent to a fluid with a quantum potential [35], and Feynman explained circulation quantisation in superfluid helium in units of h/m [36]. Couder and Fort demonstrated single-particle interference with walking droplets at macroscopic scale [37]. Kleinert developed a multivalued-field theory describing electromagnetism and gravitation as defect theories of a "world crystal" [38].

Table 1. Comparison of related medium frameworks

Framework	Preferred frame	Gravitation	Electromagnetism	Matter	Empirical status
Spin Theory [9]	Yes; photons at rest	Le Sage push	Analogue of gravity, qualitative	Spin density	Multiple conflicts (Sect. 3)
Lorentz aether [13]	Yes; undetectable	None	Maxwell	Lorentz electron	Equivalent to SR
Einstein–aether [7]	Yes; dynamical	GR + vector	Maxwell	Standard fields	Tightly constrained [8]
Analogue gravity [3]	Yes; laboratory	Acoustic metric	Not direct	Phonons, quasi-particles	Observed in laboratory [23]
Helium universe [4]	Yes; superfluid	Emergent	Emergent	Fermionic quasi-particles	Analogue model
ESMT (this work)	Yes; CMB frame (E8)	PG–Doran flow	MacCullagh rotational elasticity	Topological solitons, quantised vortices	Equivalent to GR + Maxwell where tested

3. The source theory and its critical audit

This section summarises the audit of the source theory [9], because its outcome determines what ESMT keeps, modifies or discards. Labels S0–S8 denote the axioms of the source theory as restructured in an earlier analysis [39]; the excluded claims are collected in Table A1 (Appendix A).

3.1 Velocity-relation law (S5)

The law states that the relative velocity of two systems is the hypotenuse of an isosceles right triangle whose legs are "component velocities", $v_{td}=v\sqrt{2}$. The starting relation $V=v\sqrt{1-V^2/v^2}$ admits only the solution $V=v/\sqrt{2}$, so for $v=c$ one obtains $\sqrt{1-V^2/c^2}=1/\sqrt{2}$, a constant rather than a function of velocity. Measured Lorentz factors vary continuously, from $\gamma=29.3$ for muons in a storage ring [40] down to $\gamma-1\approx\frac{1}{2}v^2/c^2\approx5.6\times10^{-16}$ for an ion clock moving at 10 m/s [41]. Moreover, the decomposition into two equal orthogonal components is not unique in three dimensions, and elsewhere the source manuscript uses a collinear decomposition, $v_{AB}/2$, which is inconsistent with it. Decision: discarded as a law. The intuition that relative motion reduces to motion relative to the medium is retained and realised correctly in Theorem 3.

3.2 Radiation-distribution law (S6)

With $n=N/4\pi R^2$ and $R=ct$ one obtains $dn/dt=-2nc/R$; the source drops the factor 2 by appeal to "symmetry". For a stationary source $\partial n/\partial t=0$ at a fixed point, whereas a moving observer measures $dn/dt=\mathbf{v}\cdot\nabla n$, which depends on velocity, contrary to the content of the law. The chain of reasoning ends in $c+v=c-v$, valid only for $v=0$. Decision: replaced by a covariant wave equation (axiom E3).

3.3 Mass, energy and dimensions (S2)

Mass is defined as a count of spins, yet it appears in $F=Ma$ with F in newtons, while the "force" $F=-c^2$ has dimensions of $m^2{\cdot}s^{-2}$. The relation $E=Mc^2$ is derived from the definition $m=c/R$ and is therefore an identity; at the same time m is treated as a constant ≈1569 rad/s to keep G fixed, corresponding to a characteristic radius $c/m\approx191$ km. The two usages are mutually incompatible. Decision: mass is excitation energy divided by c^2 (axiom E6); $E=mc^2$ follows from emergent Lorentz invariance.

3.4 Push gravity (S4)

The gravitational mechanism of the source theory belongs to the Le Sage family. For an isotropic flux of specific intensity I_s and mass absorption coefficient κ, the force between two optically thin bodies is, up to a geometric factor of order unity,

$$F=\frac{\kappa^2 I_s}{c}\,\frac{M_1M_2}{R^2},\qquad G=\frac{\kappa^2 I_s}{c}. \tag{1}$$

Lunar laser ranging limits gravitational shielding to $\kappa\lesssim10^{-22}\,m^2.k^{-1}$ [42].

Then $I_s=Gc/\kappa^2\approx2.0\times10^{42}\ Wm^{-2}sr^{-1}$, and

$$P_\oplus=4\pi I_s\kappa M_\oplus\approx1.5\times10^{46}\ W,\qquad a_{drag}\approx\frac{4\pi I_s\kappa v_{orb}}{c^2}\approx8\times10^{8}\ m\,s^{-2}, \tag{2}$$

where $P_\oplus$ is the power absorbed by the Earth (3.9×10^{19} solar luminosities) and a_{drag} is the Doppler drag at an orbital speed of 30 km/s. Since $P\propto1/\kappa$ and $a_{drag}\propto1/\kappa$, lowering κ worsens both; raising κ violates the shielding bound. (An earlier estimate [39] gave $a_{drag}\sim10^4\ m.s^{-2}$; the recalculation is about five orders of magnitude larger and strengthens the conclusion.) Decision: discarded entirely. The intuition that gravity is an action of the medium is retained in the form of a flow (Section 5.2).

This rigorous recalculation showing drag acceleration $a_{drag} \sim 8 \times 10^8$ m s^{-2}, about five orders of magnitude larger than preliminary estimates [39] demonstrates the necessity of quantitative auditing over qualitative rhetoric when evaluating heterodox physical proposals.

3.5 Instantaneous images and simultaneous extinction (S7)

Cavity ring-down spectroscopy directly measures light persisting between two mirrors after the source is switched off, with lifetime $\tau = L/[c(1-\mathcal{R})]$, about 33 μs for $\mathcal{R} = 0.9999$ and $L = 1$ m [43]. Lunar laser ranging records a round-trip time of ≈2.5 s in every measurement [44]. Decision: discarded.

3.6 Euclidean space, gyroscopes and clocks (S0)

Gravity Probe B measured a geodetic drift of 6601.8 ± 18.3 mas/yr and a frame-dragging drift of 37.2 ± 7.2 mas/yr of its gyroscope axes [45], contrary to the claim that a gyroscope axis is an absolute straight line in Euclidean space. GPS permanently compensates a rate offset of ≈ +38.6 μs/day between satellite and ground clocks [46], contrary to the claim that clocks at equal distance from the Earth's centre run at equal rates. Decision: Euclidean slices and absolute time are retained in Painlevé–Gullstrand form, which is exact, but clocks and gyroscopes respond to motion relative to the medium (Sections 5.2–5.4). Both GPS and Gravity Probe B then become confirmations rather than refutations.

3.7 Electromagnetism, atoms, thermodynamics and cosmology (S8 and corollaries)

Direct current is distributed over the whole cross-section of a conductor ($R = \rho L/A$), not only at its surface. The shell structure 2q,4q,8q does not reproduce the shell capacities $2n^2$. The temperature scale $T \in [0,1]$ is incompatible with Planck's law. Non-expansion redshift is excluded by supernova time dilation [47] and by the blackbody spectrum of the cosmic microwave background (CMB) [48]; a universe with a centre conflicts with CMB isotropy and with bounds on cosmic vorticity [49]. Decision: electromagnetism is rebuilt on MacCullagh's model (Section 5.5), matter on solitons and quantised vortices (Section 5.6), thermodynamics retains standard statistics with radiance conservation (Section 5.7), and cosmology becomes a Hubble flow (Section 5.8).

Table 2. Reconstruction decisions for each component of the Spin Theory

Original component	Problem	Decision	Replacement in ESMT
Euclidean space, absolute time	Conflicts with GP-B and GPS if read naively	Keep, make precise	Flat PG slices, free-fall time (E1, E4)
Static spin medium	No dynamics defined	Keep, add dynamics	Medium with velocity field **v** (E2)
Spin $\omega = v/R$	Correct dimension but non-local	Keep, redefine	$\boldsymbol{\Omega} = \frac{1}{2}\nabla \times \mathbf{v}$ (E2)
Velocity-relation law (S5)	Geometric identity	Discard	Clock-rate relation (11)
Radiation-distribution law (S6)	Algebraic error	Discard	Covariant wave equation (E3)
Le Sage push gravity	Energy budget, drag	Discard	Non-absorptive inflow (E4)
Inertia from the medium	Qualitative	Keep	Free fall = co-moving drift (Theorem 2)
Lensing as refraction	Requires achromaticity	Keep	Gordon optical metric (Sect. 5.5)
Magnetic and electric spin	Qualitative	Keep, make precise	$\mathbf{B} \propto \nabla \times \boldsymbol{\xi}$, MacCullagh (E5)
Instantaneous images	Refuted	Discard	Propagation at c relative to medium

Original component	Problem	Decision	Replacement in ESMT
Radiation temperature independent of distance	Conflates two concepts	Keep in part	Brightness-temperature conservation (Theorem 4)
Centred spherical universe, cyclic Big Bang	Conflicts with CMB	Discard	Centre-free Hubble flow (Sect. 5.8)

4 Construction of the Extended Spin-Medium Theory

4.1 Design principles

Six principles govern the construction, each answering a group of objections raised in Section 3.

D1, ontological fidelity. Retain the three pillars of the source theory: Euclidean space, absolute time, and the spin medium as the only physical substance.

D2, dimensional consistency. Every quantity has a definite SI dimension; counts are never used in place of mass.

D3, emergent Lorentz invariance. A preferred frame may exist but must be undetectable at the tested precision; in the present continuum formulation this is implemented through the universal-cone postulate E3 rather than derived from the microstructure (Section 5.1).

D4, no absorption. Gravity does not arise from absorption of momentum from an isotropic flux, which removes the Le Sage paradoxes.

D5, quantitative reproduction. Every measured effect must be computed numerically with error smaller than the experimental uncertainty.

D6, falsifiability. Every assumption beyond standard physics must be tied to at least one measurable parameter.

4.2 Axioms

E1, Euclidean space and absolute time. There exist global coordinates (t,x) in which the slices $t=$ const are Euclidean E^3 and t is the proper time of the medium elements. This holds exactly for vacuum and marginally bound spherically symmetric configurations (the Schwarzschild exterior, the Reissner–Nordström exterior and marginally bound Lemaître–Tolman dust) and for spatially flat cosmology; for general configurations it holds to first post-Newtonian order (Section 8.3). Inside static matter with non-zero pressure the slices can still be chosen flat, but a lapse function $N\neq 1$ multiplies c^2dt^2 in (4) below, and t is then no longer the proper time of the medium elements; none of the tests considered in this paper probes that regime.

E2, the spin medium. Space is filled by a continuous medium with velocity field $v(t,x)$ measured in E^3. The spin of the medium at a point is the local angular velocity of the medium element,

$$\boldsymbol{\Omega}(t,\mathbf{x})\equiv\frac{1}{2}\,\nabla\times\mathbf{v}(t,\mathbf{x}) \qquad \left[\mathrm{rad\,s^{-1}}\right]. \qquad (3)$$

This retains the angular-velocity dimension of "spin" in the source theory, but makes it a local, directed and measurable quantity.

E3, universal propagation cone. All excitations of the medium (light, matter, gravitational waves) obey hyperbolic equations with a common characteristic cone: speed c relative to the local medium element. Equivalently, they propagate on the effective metric

$$ds^2=-c^2\,dt^2+|d\mathbf{x}-\mathbf{v}\,dt|^2. \qquad (4)$$

E4, flow dynamics. The flow is determined by the energy–momentum distribution of matter through the Einstein field equations written in flow variables. In spherical symmetry, for vacuum and for marginally bound dust, this reduces to the exact relation

$$v^2(r) = \frac{2G\,m(r)}{r}, \qquad (5)$$

where $m(r)$ is the Misner–Sharp mass within radius r [29,50]. In the Newtonian limit $\frac{1}{2}v^2 = -\Phi_N$.

E5, electromagnetism as rotational elasticity. On top of the flow, the medium admits small displacements $\boldsymbol{\xi}(t,\mathbf{x})$ whose elastic energy depends only on the rotation $\nabla\times\boldsymbol{\xi}$ (MacCullagh aether). The electromagnetic vector potential is $\mathbf{A} = \beta\boldsymbol{\xi}$, with β a conversion constant.

E6, matter as topological structure. Material particles are stable localised topological configurations of the medium (solitons, quantised vortices). The inertial mass of a system is its total energy divided by c^2, binding energy included.

E7, microstructure. The medium has a microscopic length scale l. For wavelengths $\lambda \gg l$, E3 holds exactly; for $\lambda \sim l$ the dispersion relation acquires corrections

$$\omega^2 = c^2k^2\left[1 + \zeta_1(kl) + \zeta_2(kl)^2 + \dots\right]. \qquad (6)$$

E8, cosmic rest frame. Averaged over cosmological scales, the rest frame of the medium coincides with the frame in which the CMB is isotropic.

E1, E2 and E8 realise directly the axioms S0 and S1 of the source theory. E3 replaces S6; E4 replaces the Le Sage mechanism; E5 makes "magnetic spin" precise; E6 replaces the definition of mass as a count. E7 and E8 are new assumptions beyond standard physics, and are where the theory can fail.

Classification of Theoretical Foundations: To ensure complete methodological transparency, the components of ESMT are categorized as follows: Inherited/Reconstructed Physics (Axioms E1–E6): These axioms do not constitute an independent fundamental derivation of gravity from microscopic principles. Rather, Axiom E4 adopts the energy-momentum field equations of GR written in flow variables, yielding the Painlevé–Gullstrand form of the Schwarzschild solution (Eq. 9) and MacCullagh's representation of electrodynamics (E5). Their mathematical consequences (e.g., geodetic motion, Shapiro delay, gravitational lensing) are directly inherited from GR and Maxwell theory. Physical Hypotheses (H1–H2): Hypotheses H1 (electric charge as quantised rotational defects) and H2 (matter as topological solitons) are structural conjectures inspired by defect mechanics [38] and Skyrme theory [31]. They provide qualitative mechanistic models but are not derived from an underlying quantum field dynamics. Genuinely Independent Postulates (Axioms E7–E8): Axioms E7 (microscopic dispersion scale l) and E8 (CMB-fixed preferred frame) represent independent physical assumptions beyond standard relativity. These two axioms break exact Lorentz invariance at high energies and provide the sole foundation for the falsifiable predictions (F1–F4) of ESMT.

4.3 Kinematics of the medium and the spin decomposition

By the Helmholtz theorem, any sufficiently smooth velocity field decaying at infinity splits into irrotational and solenoidal parts,

$$\mathbf{v} = -\nabla\psi + \nabla\times\boldsymbol{\chi}, \qquad \boldsymbol{\Omega} = \frac{1}{2}\nabla\times(\nabla\times\boldsymbol{\chi}). \qquad (7)$$

In ESMT the irrotational part carries the gravitational effect of static mass (radial inflow), and the solenoidal part carries the gravitational effect of moving and rotating mass (gravitomagnetism). The spin $\boldsymbol{\Omega}$ is non-zero only in the solenoidal part. This gives a precise meaning to the distinction between "scalar

spin" and "directed spin" in the source theory: scalar spin corresponds to isotropic irrotational inflow, directed spin to vorticity Figure 1).

Small perturbations $\boldsymbol{\xi}$ on the background $\mathbf{v}$ carry electromagnetism (E5). The total velocity of a medium element is $\mathbf{v}+\dot{\boldsymbol{\xi}}$ and its total spin is $\Omega_{\text{tot}}=\Omega+\frac{1}{2}\nabla\times\dot{\xi}$. Gravitation and electromagnetism are thus two scales of one motion: a large-scale mean flow and small-scale rotational oscillations.

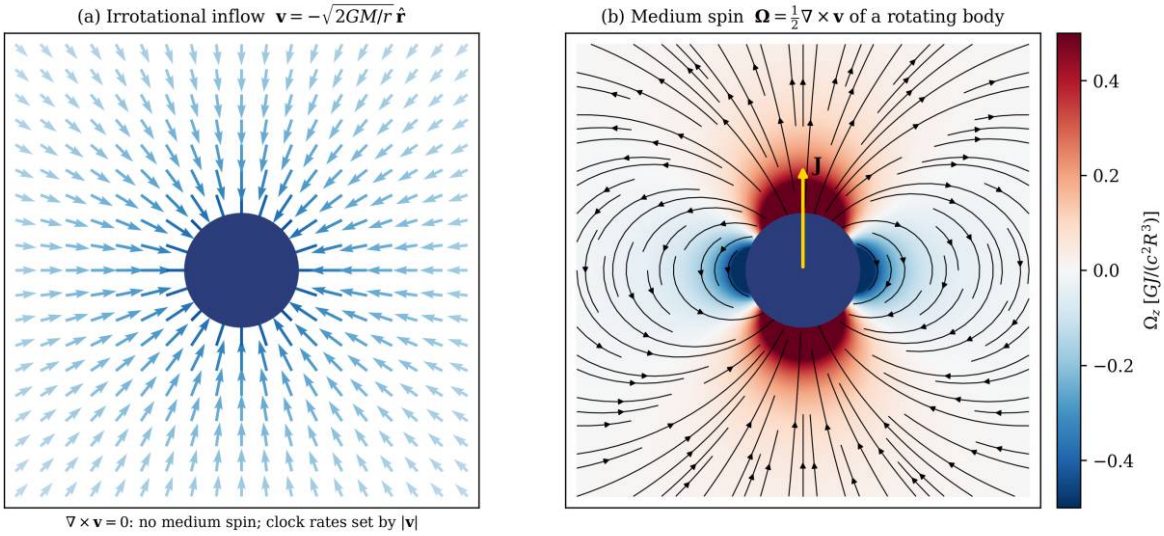


Figure 1. The ESMT picture. (a) A static mass induces an irrotational inflow of the medium at the Newtonian escape speed; clock rates depend only on the speed relative to this flow (Theorem 3). (b) A rotating body adds a solenoidal component; the medium spin $\boldsymbol{\Omega}=\frac{1}{2}\nabla\times\mathbf{v}$ (field lines and colour, meridional plane, J vertical) has a dipolar pattern and coincides with the Lense–Thirring precession rate (16).

5 Results

5.1 Emergent Lorentz invariance and time dilation as a dynamical effect

Theorem 1 (Emergent Lorentz invariance). Suppose that in some region the medium moves uniformly, $\mathbf{v}=$ const, that all physical fields satisfy E3, and that the lower-order terms of their field equations are Lorentz covariant. Then every result obtained with rods and clocks built from those fields is invariant under the Lorentz group, and no local experiment can determine $\mathbf{v}$.

Proof (sketch; full proof in Appendix C.1). The change of coordinates $x'=x-vt$ brings (4) to the Minkowski form $ds^2=-c^2dt^2+d\mathbf{x}'^2$. Hyperbolic equations whose principal symbol is $\eta^{\mu\nu}k_\mu k_\nu$ have a symmetry group containing the Lorentz group of η. A rod (an equilibrium configuration of the fields) and a clock (a periodic solution) at rest in K' are mapped by a Lorentz transformation into a valid rod and clock moving at any velocity $w<c$; measured quantities (ratios of lengths, ratios of periods, the measured speed of light) are therefore independent of w, including $w=-v$. ▫

Theorem 1 formalises Bell's argument [16]: a moving clock runs slow not because "time contracts" in a metaphysical sense, but because its internal dynamics, which are dynamics of the medium, change when it moves relative to the medium. This is precisely the source theory's intuition that "processes slow down rather than time contracting", now derived from E3 rather than merely asserted; the theorem also explains why all clocks slow by the same factor.

The light clock gives the most transparent example. Two mirrors a distance L apart move with speed w perpendicular to their axis relative to the medium. Since light travels at c relative to the medium, in a

half-period $\Delta t/2$ it covers $c\Delta t/2$ along the hypotenuse of a right triangle with legs L and $w\Delta t/2$:

$$\left(\frac{c\,\Delta t}{2}\right)^2 = L^2 + \left(\frac{w\,\Delta t}{2}\right)^2 \Rightarrow \Delta t = \frac{2L/c}{\sqrt{1-w^2/c^2}}. \qquad (8)$$

The right triangle with hypotenuse c that the source theory places at the centre of its velocity-relation law appears here in its correct role: one leg is the arbitrary speed w of the clock relative to the medium, the other is $c\sqrt{1-w^2/c^2}$. The triangle is isosceles only in the special case $w=c/\sqrt{2}$, i.e. $\gamma=\sqrt{2}$.

Scope and Pedagogical Basis of Theorem 1: We emphasize that Theorem 1 does not constitute a microscopic derivation of Lorentz invariance from atomic or lattice medium constituents. Rather, it is a formalization of Bell's dynamical interpretation of special relativity [16]: assuming that all physical fields share a common characteristic wave speed c relative to the local medium (Axiom E3) and that the field equations are Lorentz-covariant, moving bound states (rods) and periodic modes (clocks) necessarily undergo physical contraction and slowing. Emergent Lorentz invariance is thus built into the continuum formulation as a working postulate (E3) rather than derived from an explicit microstructural dynamic.

5.2 Gravitation as flow of the medium

For a spherical body of mass M, (5) gives the radial inflow $\mathbf{v} = -\sqrt{2GM/r}\,\hat{\mathbf{r}}$. Substituting into (4),

$$ds^2 = -c^2dt^2 + \left(dr + \sqrt{\frac{2GM}{r}}\,dt\right)^2 + r^2\left(d\theta^2 + \sin^2\theta\, d\varphi^2\right). \qquad (9)$$

This is exactly the Schwarzschild metric in Painlevé–Gullstrand coordinates [27,28]: the transformation

$$t = t_S + f(r), \qquad f'(r) = \frac{\sqrt{2GM/r}}{c^2 - 2GM/r}, \qquad (10)$$

brings (9) to the familiar Schwarzschild form. All coordinate-independent consequences of the Schwarzschild solution are therefore reproduced exactly. The slices $t=$ const are flat E^3 (E1 holds exactly), and t is the proper time of observers falling from rest at infinity. We stress that this is a re-articulation of a known exact solution of GR within a medium ontology, obtained because E4 adopts the Einstein field equations in flow variables; it is not an independent derivation of gravitation from medium microphysics.

Theorem 2 Free fall is co-moving drift. A test body released from rest at infinity has coordinate velocity $d\mathbf{x}/dt = \mathbf{v}$ at every point, and its proper time equals t. Free fall is therefore independent of composition (weak equivalence principle), and a freely falling body experiences no force.

Proof. With $d\mathbf{x} = \mathbf{v}\,dt$, (4) gives $ds^2 = -c^2dt^2$, i.e. $d\tau = dt$. Direct substitution shows that this curve satisfies the geodesic equation of (9) with specific energy $E/mc^2 = 1$ (Appendix C.2). Since the geodesic contains no material parameter, the weak equivalence principle holds. ▫

Theorem 2 is the precise form of the source theory's claims that "in free fall the net force vanishes" and that "inertia is a reaction to the medium". On this view, inertia is resistance to being forced away from co-motion with the medium. MICROSCOPE confirms composition independence to 10^{-15} [51], and lunar laser ranging confirms that gravitational self-energy falls in the same way [25].

Theorem 3 Clock rate is fixed by speed relative to the medium. An ideal clock with coordinate velocity $\mathbf{u} = d\mathbf{x}/dt$ in a medium with velocity $\mathbf{v}$ ticks at the rate given by Eq. (11) below, where $w = |\mathbf{u} - \mathbf{v}|$ is its speed relative to the local medium.

$$\frac{d\tau}{dt}=\sqrt{1-\frac{|\mathbf{u}-\mathbf{v}|^2}{c^2}}\equiv\sqrt{1-\frac{w^2}{c^2}}. \qquad (11)$$

Proof. Substitute $d\mathbf{x}=\mathbf{u}\,dt$ into (4). ▫

Relation (11) is exact (no approximation) for the Schwarzschild field and unifies effects that standard presentations treat separately:

Clock at rest in a gravitational field ($\mathbf{u}=0$): the medium streams past it at $w=\sqrt{2GM/r}$, giving $d\tau/dt=\sqrt{1-2GM/rc^2}$, the exact Schwarzschild redshift.

Clock moving where there is no mass ($\mathbf{v}=0$): $w=u$, giving special-relativistic time dilation.

Clock on a circular orbit: the orbital velocity $u=\sqrt{GM/r}$ (exact in Schwarzschild, and hence Painlevé–Gullstrand, time at fixed r) is perpendicular to the radial inflow $\sqrt{2GM/r}$, so that $w^2=3GM/r$ and

$$\frac{d\tau}{dt}=\sqrt{1-\frac{3GM}{rc^2}}, \qquad (12)$$

which is the exact GR result for circular orbits.

Light: $w=c$. Horizon: where $v=c$, i.e. $r=2GM/c^2$; inside, the medium flows faster than c and nothing can move upstream.

In the circular-orbit case the speed relative to the medium is the hypotenuse of a right triangle whose legs are the orbital speed and the inflow speed. The source theory's geometric intuition that "relative velocity is the hypotenuse of a right triangle" thus has an exact realisation, although the triangle is not isosceles.

5.3 Quantitative consequences

GPS. A ground clock on the equator ($R_\oplus=6.3781\times10^6$ m, rotational speed 465 m/s) and a GPS satellite clock ($r_s\approx2.656\times10^7$ m, $u_s=3874$ m/s) have speeds relative to the medium

$$w_\oplus^2=v_{rot}^2+\frac{2GM_\oplus}{R_\oplus}, \qquad w_s^2=u_s^2+\frac{2GM_\oplus}{r_s}. \qquad (13)$$

Inserting into (11) and taking the ratio, the accumulated offset per day is $+38.54\ \mu s$ for a spherical Earth, composed of $+45.65\ \mu s$ from the inflow and $-7.11\ \mu s$ from motion. Including the Earth's oblateness yields $+38.576\ \mu s$/day (Section 6.3), matching the value compensated in the system [46]. Figure 2 shows the decomposition as a function of orbital radius; the net offset vanishes at $r\approx1.50\,R_\oplus$.

Light deflection and delay. Light satisfies $|\mathbf{u}-\mathbf{v}|=c$. Because (9) is the Schwarzschild solution, photon orbits obey the Binet equation

$$\frac{d^2u}{d\varphi^2}+u=\frac{GM}{h^2}\sigma+\frac{3GM}{c^2}u^2, \qquad u=1/r, \qquad (14)$$

with $\sigma=0$ for light and $\sigma=1$ for massive bodies of specific angular momentum h. Numerical integration (Appendix D) gives a deflection at the solar limb of $1.75120''$, in agreement with the analytic $4GM/bc^2$ to 10^{-5} and with VLBI and Cassini, which constrain the post-Newtonian parameter to $\gamma-1=(2.1\pm2.3)\times10^{-5}$ [52]. The round-trip Shapiro delay for Earth–Saturn geometry at impact parameter $1.6R_\odot$ is $\approx264\ \mu s$ [52,53]. In the language of the source theory the ray is "refracted" by the flow, with effective index $n_{eff}=c/|d\mathbf{x}/dt|$; because all excitations share one cone (E3), the deflection is achromatic, as observed.

Planetary orbits. For massive bodies (14) gives a perihelion advance per orbit of $6\pi GM/\left[c^2a\left(1-e^2\right)\right]$.

Direct integration for Mercury yields $42.98''$/century.

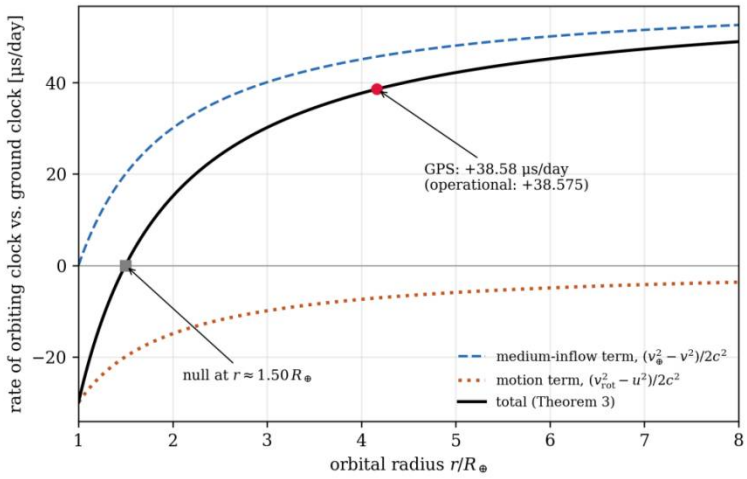


Figure 2. Rate of a clock on a circular equatorial orbit relative to a clock on the equatorial geoid, from Theorem 3 with Earth's J_2 included.

The medium-inflow term (dashed) and the motion term (dotted) have opposite signs, and the net offset vanishes at $r \approx 1.50\,R_\oplus$; at the GPS radius the total is $+38.576\ \mu s/day$, against the operational value $+38.575\ \mu s/day$ [46].

5.4 Medium spin and gravitomagnetism

A body with angular momentum $\mathbf{J}$ drags the medium into vortical motion. In the weak, slow-motion field, the off-diagonal metric component of a rotating body is $g_{0i} = -\left(2G/c^3\right)(\mathbf{J}\times\mathbf{x})_i / r^3$ [1,54]. Comparing with the cross term $-2\mathbf{v}\cdot d\mathbf{x}\,dt$ of (4) identifies the solenoidal part of the flow,

$$\mathbf{v}_{vort} = \frac{2G}{c^2}\,\frac{\mathbf{J}\times\mathbf{r}}{r^3}. \qquad (15)$$

By definition (3), the spin of the medium is

$$\boldsymbol{\Omega} = \frac{1}{2}\nabla\times\mathbf{v}_{vort} = \frac{G}{c^2 r^3}\,[3(\mathbf{J}\cdot\hat{\mathbf{r}})\hat{\mathbf{r}} - \mathbf{J}]. \qquad (16)$$

Expression (16) coincides exactly with the Lense–Thirring (frame-dragging) precession rate of a gyroscope [1,45].

Proposition 1 Gyroscopes follow the medium spin. In the weak field, the axis of a free gyroscope immersed in the medium rotates with the local medium element at angular velocity $\boldsymbol{\Omega} = \frac{1}{2}\nabla\times\mathbf{v}$, plus a geodetic (de Sitter) term arising from the gyroscope's orbital motion through the spatially varying radial inflow.

Proposition 1 restores, in correct form, the source theory's definition of a straight line as "the line along the axis of a free gyroscope": the axis is fixed not relative to abstract Euclidean space but relative to the local medium element. Gravity Probe B measured 37.2 ± 7.2 mas/yr for frame dragging (prediction 39.2) and 6601.8 ± 18.3 mas/yr for the geodetic effect (prediction 6606.1) [45]; analysis of the nodes of the LAGEOS satellites gave frame dragging in agreement at about the 10% level [55]. In ESMT language these experiments are direct measurements of the spin of the spatial medium, an outcome that the source theory anticipated intuitively ("space has spin") but expressed in a way that led to its refutation. Hamilton and Lisle already noted that the Kerr river carries a twist [29]; Proposition 1 makes explicit its weak-field identification with the measured gyroscope precession and with the angular velocity of the

medium element (Figure 1b).

Order of magnitude: at the Earth's pole, (16) gives $\Omega \approx 2GJ_\oplus/c^2R_\oplus^3 \approx 3.4\times10^{-14}$ rad/s, or about 220 mas/yr, about nine orders of magnitude below the Earth's rotation rate.

Physical Interpretation and Observational Distinctions: In standard GR, the Lense–Thirring effect is understood geometrically as the precession of a parallel-transported spin vector in a curved spacetime background. ESMT provides a mechanical counterpart: the rotating mass exerts a shear torque on the physical medium, inducing a solenoidal velocity field v_{vort} (Eq. 15). The local medium spin $\Omega = \frac{1}{2}\nabla\times v_{vort}$ is the literal physical angular velocity of the medium continuum.

In the weak-field regime, this physical velocity field yields predictions identical to GR for Gravity Probe B (39.2 mas/yr) and LAGEOS [45, 55]. However, the physical medium interpretation allows for observable departures from standard GR under two specific conditions: (i) High-frequency/Strong-field limits: If the medium exhibits rotational elasticity modulus K or microstructural cutoff l (E7), high-frequency gravitational waves passing through a rotating background will experience spin-dependent dispersion or polarization rotation not present in pure GR. (ii) Analogue systems: In laboratory condensed-matter analogues (such as vortex states in BECs or superfluid helium), the medium spin $\boldsymbol{\Omega}$ directly couples to quasiparticle spin states, providing a testable physical mechanism where geometric frame-dragging and real hydrodynamical vorticity can be independently calibrated.

5.5 Electromagnetism as rotational elasticity of the medium

By E5, the Lagrangian density of rotational perturbations in the local rest frame of the medium (in the temporal gauge, $A_0=0$, appropriate to source-free fields) is

$$\mathcal{L} = \frac{1}{2}\rho_m\dot{\boldsymbol{\xi}}^2 - \frac{1}{2}K(\nabla\times\boldsymbol{\xi})^2, \qquad \nabla\cdot\boldsymbol{\xi}=0, \qquad (17)$$

with ρ_m the inertial density and K the rotational elastic modulus. The Euler–Lagrange equation is $\rho_m\ddot{\boldsymbol{\xi}} = -K\nabla\times(\nabla\times\boldsymbol{\xi})$. Define $A=\beta\xi$, $E=-\partial_t A$, $B=\nabla\times A$. Then $\nabla\times E=-\partial_t B$ and $\nabla\cdot B=0$ hold identically, and the equation of motion becomes

$$\nabla\times B = \frac{\rho_m}{K}\frac{\partial E}{\partial t}, \qquad \nabla\cdot E=0. \qquad (18)$$

Matching the energy density $\frac{1}{2}\rho_m\dot{\boldsymbol{\xi}}^2 + \frac{1}{2}K(\nabla\times\boldsymbol{\xi})^2$ with $\frac{1}{2}\varepsilon_0E^2 + B^2/2\mu_0$ gives $\rho_m=\varepsilon_0\beta^2$ and $K=\beta^2/\mu_0$, hence the speed of rotational waves

$$c_{EM} = \sqrt{K/\rho_m} = 1/\sqrt{\varepsilon_0\mu_0}. \qquad (19)$$

Maxwell's vacuum equations are thus the equations of elastic rotational oscillation of the medium. The local rotation angle of a medium element is $\theta = \frac{1}{2}\nabla\times\xi = B/2\beta$: the magnetic field is the "rotation" of the medium, which gives the "magnetic spin" of the source theory its precise definition. Faraday's law then reads: the rotation rate of a medium element is $\dot{\theta} = -\nabla\times E/2\beta$.

Light in a flowing medium. When the background flows with $\mathbf{v}$, rotational waves propagate on Gordon's optical metric [56]. For unit intrinsic refractive index (vacuum), the Gordon metric reduces to the background metric (4); light therefore shares the cone of all other excitations and gravitational deflection is achromatic. Universality E3 here is the condition $c_{EM}=c$, i.e. that the rotational wave speed equals the common limiting speed. GW170817 confirms $|c_{GW}-c_{EM}|/c \lesssim 10^{-15}$ [24].

Sources: electric charge. With $\nabla\cdot\boldsymbol{\xi}=0$, (18) describes only free fields. In the defect theory of elastic media

[38], sources of rotational fields are topological defects (rotational dislocations). We formulate hypothesis H1: electric charge is the endpoint of a rotational defect of the medium carrying quantised rotational flux. H1 explains naturally why charge is quantised and conserved (a topological invariant) but not the mass ratios of charged particles; this remains open (Section 8.3).

Currents. For direct current in a wire the standard model is retained: the current is distributed uniformly over the cross-section and concentrates at the surface only at high frequency (skin depth $\delta=\sqrt{2\rho/\omega\mu}$). The corresponding claim of the source theory is discarded.

Theoretical Scope and Limitations of the Electromagnetic Model: The mapping between MacCullagh's rotational elasticity and Maxwell's equations (Eqs. 17–19) is strictly valid for source-free fields in vacuum under the temporal gauge choice ($A_0=0$). While it offers a visual mechanical representation where $E=-\dot{A}$ represents translation velocity and $B=\nabla\times A$ represents rotational strain of the medium, it does not constitute a full gauge-invariant field theory. Furthermore, Hypotheses H1 (charge as rotational defects) and H2 (particles as topological solitons) are structural conjectures. ESMT does not derive the electroweak gauge symmetry $SU(2)\times U(1)$, quantization of electric charge from first principles, or the fermion mass hierarchy. These concepts are included strictly to demonstrate qualitative compatibility with particle physics concepts, and must not be interpreted as established mathematical derivations of the theory.

5.6 Matter and quanta: quantised vortices of the medium

Following Madelung [35], with $\psi=\sqrt{\rho}\,e^{iS/\hbar}$ the Schrödinger equation is equivalent to the fluid system

$$\partial_t\rho+\nabla\cdot(\rho\mathbf{v})=0, \qquad m\left(\partial_t+\mathbf{v}\cdot\nabla\right)\mathbf{v}=-\nabla(V+Q), \qquad Q=-\frac{\hbar^2}{2m}\frac{\nabla^2\sqrt{\rho}}{\sqrt{\rho}}, \tag{20}$$

with $\mathbf{v}=\nabla S/m$. The velocity field is irrotational except on nodal lines of ψ, where circulation is quantised:

$$\Gamma=\oint\mathbf{v}\cdot d\mathbf{l}=n\,\frac{h}{m}, \qquad n\in\mathbb{Z}. \tag{21}$$

In ESMT, (21) reads: the spin of the matter medium is quantised in units of h/m. A vortex of winding number n carries angular momentum $n\hbar$ per particle, as in superfluid helium [36]. This connects the classical notion of spin as angular velocity in the source theory with Planck's constant: the product of angular velocity and area (the circulation) is quantised. Wallstrom [57] showed that (20) is equivalent to the Schrödinger equation only when (21) is added as an independent postulate; ESMT accepts (21) as part of E6 (single-valuedness of the medium phase).

Through the Madelung–Schrödinger equivalence, ESMT inherits non-relativistic quantum mechanics in full: the Rydberg spectrum of hydrogen, the shell capacities $2n^2$ (once intrinsic spin is included through the Pauli equation), and the uncertainty principle. The latter follows from describing the medium by a wave field: the Fourier bound $\Delta x\,\Delta k\geq\frac{1}{2}$ together with $p=\hbar k$. The source theory rejects this principle; in ESMT it is a natural consequence of the wave nature of the medium.

Spin one-half and baryons. A single vortex has integer angular momentum in units of $\hbar$. Half-integer spin requires a different topological structure: Finkelstein and Rubinstein [33] proved that solitons can be quantised as fermions when the fundamental group of configuration space has a suitable element of order two; Skyrme [31] and Witten [32] showed that baryons can be described as solitons of the meson field, and Faddeev and Niemi found stable knotted solitons [34]. ESMT proposes (hypothesis H2) that elementary particles are topological solitons of the spin medium, with half-integer spin arising by the

Finkelstein–Rubinstein mechanism. Reproducing the mass spectrum and gauge group of the Standard Model is beyond the scope of this paper.

Binding energy. By E6, the mass of a nucleus equals the total energy of the soliton configuration divided by c^2, so negative binding energy reduces mass (the mass defect). The binding-energy curve per nucleon, peaking near 8.8 MeV around ^{56}Fe-^{62}Nii, is a test of soliton models of nuclei that has been studied within the Skyrme framework.

5.7 Radiation thermodynamics

The rotational modes of the medium in a cavity of volume V have mode density $8\pi\nu^2 V/c^3$. Quantising each mode with energy $h\nu$ at thermal equilibrium yields Planck's law and the Wien and Stefan–Boltzmann laws. The temperature scale is the thermodynamic (kelvin) scale; the scale $T\in[0,1]$ of the source theory is discarded.

Theorem 4 Conservation of brightness temperature. Along a ray in a non-absorbing medium, I_ν/ν^3 is conserved. The brightness temperature T_b of blackbody radiation is therefore independent of distance when there is no frequency shift between source and observer, and transforms as $T_{obs}=T_{em}/(1+z)$ under a frequency shift $1+z$.

Proof. I_ν/ν^3 is proportional to the photon occupation number in phase space, which is invariant by Liouville's theorem. A Planck spectrum at temperature T maps into a Planck spectrum at $T/(1+z)$ under frequency scaling. ▫

Theorem 4 makes precise the source theory's claim that "the temperature of thermal radiation does not depend on distance from the source": it holds for brightness temperature, not for the equilibrium temperature of an absorbing body at distance d, which is $T_\odot\sqrt{R_\odot/2d}\approx 278$ K at the Earth. The redshifted version gives $T_{CMB}(z)=T_0(1+z)$, which is observationally confirmed.

5.8 Cosmology: the Hubble flow of the medium

The flat FLRW metric $ds^2=-c^2dt^2+a^2(t)\,d\mathbf{x}^2$, with physical coordinate $\mathbf{r}=a\mathbf{x}$, becomes

$$ds^2=-c^2dt^2+|d\mathbf{r}-H(t)\,\mathbf{r}\,dt|^2, \qquad H=\dot{a}/a. \tag{22}$$

This is exactly the form (4) with the Hubble flow $\mathbf{v}=H\mathbf{r}$ in Euclidean space, and t is cosmic time, the proper time of the medium elements. ESMT therefore retains Euclidean space and absolute time on cosmological scales, provided spatial curvature vanishes; Planck 2018 measures $\Omega_k=0.001\pm0.002$ [58].

No centre. Subtracting the flow velocity at an arbitrary point $\mathbf{r}_0$ gives $\mathbf{v}-H\mathbf{r}_0=H(\mathbf{r}-\mathbf{r}_0)$: every element sees the same isotropic Hubble flow around itself. The centred spherical universe of the source theory is replaced by a homogeneous flow, consistent with the cosmological principle and CMB isotropy.

Redshift. Light moves at c relative to the expanding medium, so wavelengths stretch with a: $1+z=a_0/a_{em}$. Consequently distant processes are dilated by $1+z$, as observed in supernova light curves and spectra [47], and the CMB blackbody spectrum is preserved (Theorem 4), as measured by FIRAS [48].

Dark energy. With a cosmological constant, H tends to a constant and $\frac{1}{2}v^2=\frac{1}{2}H^2r^2$ corresponds to the potential $\Phi_\Lambda=-\Lambda c^2r^2/6$ with $H^2=\Lambda c^2/3$. In medium language, a pure cosmological constant corresponds to a stationary (de Sitter) flow with constant, uniform divergence $\nabla\cdot\mathbf{v}=3H$. ESMT does not explain the value of Λ.

Cosmic spin. Vorticity of the medium on cosmological scales would imprint characteristic anisotropic patterns on the CMB. Saadeh et al. bound cosmic vorticity to $(\omega/H)_0<4.7\times10^{-11}$ [49], a direct constraint on the spin of the medium on the largest scales.

Preferred frame. E8 identifies the mean rest frame of the medium with the CMB frame, relative to which the Solar System moves at ≈370 km/s [59]. By Theorem 1 this motion is undetectable by local experiments when E3 holds exactly; if E7 slightly violates E3, any signal must point along the CMB dipole (Section 7).

6. Quantitative confrontation with experiment

6.1 Computational method

All quantities were computed in three independent ways: analytic formulas derived from (4), (9), (11) and (16); numerical integration of the Binet equation (14) with an adaptive Runge–Kutta 4(5) scheme at relative tolerance 10^{-12}–10^{-13}; and comparison with published values. Constants: $c = 299\,792\,458$ m/s, $GM_\odot = 1.32712440018\times10^{20}$ m^3 s^{-2}, $GM_\oplus = 3.986004418\times10^{14}$ m^3 s^{-2}, $R_\odot = 6.957\times10^{8}$ m. The complete code is given in Appendix D.

6.2 Results

Table 3 compares ESMT with measurements and with the source theory. The first row illustrates the transition most clearly. From the same intuition that "the rate of a process depends on motion relative to the medium", the source theory predicts equal rates for two clocks at equal distance from the Earth's centre, whereas ESMT, with the inflow of the medium computed correctly, reproduces the GPS offset to four significant figures. The difference is that the source theory regards the medium around the Earth as static, while ESMT recognises that it flows inward at the escape speed.

Table 3. ESMT predictions compared with measurements and with the source theory (Category A: consistency checks with GR and Maxwell electrodynamics)

Quantity	ESMT relation	ESMT value	Measured	Source theory
GPS clock-rate offset	(11), (13)	+38.54 (sphere); +38.576 (with J_2) μs/day	+38.575 μs/day (factory offset) [46]	Predicts 0
Pound–Rebka redshift (22.5 m)	(11), $u=0$	2.46×10^{-15}	Agrees within 10% [60]	Not computed
Gravity Probe A (10 000 km)	(11)	GR value	Agrees to 7×10^{-5} [61]	Not computed
Muon time dilation	(8), Thm. 1	$\gamma = 29.3$	Agrees to $\sim10^{-3}$ [40]	Inserted by hand
Ion clock at 10 m/s; 33 cm lift	(11)	5.6×10^{-16}; 3.6×10^{-17}	Agrees [41]	Conflicts
Solar-limb light deflection	(14), numerical	1.75120″	$\gamma-1 = (2.1\pm2.3)\times10^{-5}$ [52]	Qualitative
Mercury perihelion advance	(14), numerical	42.98″/century	≈43″/century [1]	Not computed
Shapiro round trip ($b = 1.6R_\odot$, Saturn)	$\frac{4GM}{c^3}\ln\frac{4r_1r_2}{b^2}$	≈264 μs	Consistent [52,53]	Not computed
GP-B geodetic	Prop. 1	6606 mas/yr	6601.8 ± 18.3 [45]	Predicts 0
GP-B frame dragging (medium spin)	(16)	39.2 mas/yr	37.2 ± 7.2 [45]	Predicts 0
LAGEOS frame dragging	(16)	GR value	Agrees at ∼10% [55]	Not computed
Equivalence principle	Thm. 2	$\eta = 0$	$\eta \lesssim 10^{-15}$ [51]	Qualitatively

Quantity	ESMT relation	ESMT value	Measured	Source theory
				consistent
Speed of gravitational waves	E3	c	$\lvert\Delta c\rvert/c \lesssim 10^{-15}$ [24]	Undefined
Light in a cavity after switch-off	Propagation at c	$\tau = L/[c(1-\mathcal{R})]$	Measured, $\sim 10-30\ \mu s$ [43]	Predicts 0
Lunar laser ranging	Propagation at c	≈ 2.5 s round trip	Agrees to mm [44]	Predicts instantaneous
Supernova time dilation	(22)	$(1+z)$	Agrees [47]	Conflicts
CMB spectrum, $T(z)$	Thm. 4	Blackbody, $T_0(1+z)$	Deviation <50 ppm [48]	Conflicts
Spatial curvature	E1	$\Omega_k = 0$	0.001 ± 0.002 [58]	Consistent
Cosmic vorticity	(3) on large scales	0 (minimal)	$(\omega/H)_0 < 4.7\times10^{-11}$ [49]	Not considered

Classification of the comparisons. All entries of Table 3 belong to Category A: they are consistency checks showing that minimal ESMT (E1–E6) reproduces GR and Maxwell electrodynamics where these have been tested, and none of them can discriminate ESMT from GR. Genuinely independent tests of ESMT (Category B) arise only from the additional postulates E7 and E8 and are formulated quantitatively as predictions F1–F4 in Section 7.

6.3 Sensitivity analysis

The minimal value $+38.54\ \mu s/day$ treats the Earth as spherical. Including the quadrupole $J_2 = 1.08263\times10^{-3}$ in the equatorial potential (via $\frac{1}{2}v^2 = -\Phi_N$ with $\Phi_N = -(GM/R)\left(1+\frac{1}{2}J_2\right)$) and using the nominal semi-major axis $a = 26\,561.75$ km, ESMT gives $+38.576\ \mu s/day$. This agrees with the $+38.575\ \mu s/day$ corresponding to the factory frequency offset -4.4647×10^{-10} of GPS satellite clocks [46] to four significant figures. For deflection and perihelion advance, the relative numerical error is below 10^{-5}, far smaller than the measurement uncertainties. We stress that, since (9) is an exact solution of GR in specific coordinates, these agreements are consistency checks of the reconstruction, not independent confirmations of ESMT over GR.

7 Parameters, constraints and falsifiable predictions

Minimal ESMT (E1–E6) is empirically equivalent to GR plus Maxwell electrodynamics in all existing tests. Its content beyond standard physics resides in E7, E8, H1 and H2. Table 4 lists the characteristic parameters and current bounds.

Table 4. ESMT parameters and current experimental bounds

Parameter	Physical meaning in ESMT	Minimal value	Current bound	Source
l (with $\zeta_1 \sim 1$)	Granularity of medium; linear dispersion	0	$E_{QG,1} > 1.2E_{Pl}$, i.e. $l \lesssim l_{Pl}$	[62,63]
$\delta_{EM} = c_{EM}/c_{GW} - 1$	Non-universality between rotational and gravitational waves	0	$\lesssim 10^{-15}$	[8,24]
δ_{mat}	Non-universality between matter and light	0	$\lesssim 10^{-18}$ (anisotropy of c)	[2,19,20]

Parameter	Physical meaning in ESMT	Minimal value	Current bound	Source
α_1,α_2	Post-Newtonian effects of motion relative to preferred frame	0	$\lvert\alpha_1\rvert\lesssim 10^{-5}$, $\alpha_2\lesssim 1.6\times10^{-9}$	[1,25,26]
ω_{cos}/H_0	Medium spin on cosmological scales	0	$<4.7\times10^{-11}$	[49]
κ	Momentum absorption (Le Sage mechanism)	0	$\lesssim 10^{-22}$ m ^{2} kg $^{-1}$	[42]

Category B Genuinely Independent, Falsifiable Tests of ESMT: Quantitative Formulations of Predictions F1–F4:

F1. CMB-Locked Lorentz Violation Amplitude:

Mathematical Signal: The fractional anisotropic variation in light speed is $\delta c(\theta,t)/c = A_{ESMT}(V(t)/c)^2\sin^2\theta(t)$ (Eq. 23), where $V(t)\approx 370$ km/s is the Solar System speed relative to the CMB.

Quantitative Bound & Sensitivity: Current rotating optical cavity experiments (e.g., Nagel et al. [20]) constrain $|\delta c/c|\lesssim 10^{-18}$, which sets an upper bound $A_{ESMT}\lesssim 6.6\times10^{-13}$ (with $(V/c)^2 \approx 1.52\times10^{-6}$).

Falsification Condition: Any unambiguous detection of anisotropic light speed whose sidereal phase does not align with the CMB dipole direction ($(l,b)=(264°,48°)$) within ±2° uncertainty will strictly rule out Axiom E8.

Worked example for F1. The CMB dipole points towards (l, b) = (264°, 48°), i.e. right ascension $\alpha_D \approx 168°$ (11.2 h) and declination $\delta_D \approx -7°$ [59], with $V \approx 370$ km/s, so that $(V/c)^2 \approx 1.52\times10^{-6}$. Consider two orthogonal horizontal cavities rotating about the local vertical with angular frequency ω_r. Projecting the template (Eq. 23) onto the horizontal plane gives a fractional beat frequency

$\Delta\nu/\nu = A_{ESMT}\,(V/c)^2\sin^2\chi(t)\cos[2\omega_r t - 2\psi(t)]$,

where $\chi(t)$ is the zenith angle and $\psi(t)$ the azimuth of the dipole direction. For a laboratory at latitude φ, $\cos\chi = \sin\varphi\sin\delta_D + \cos\varphi\cos\delta_D\cos H$, with hour angle $H = LST - \alpha_D$. The signal therefore appears only at twice the rotation frequency, with an amplitude envelope $\sin^2\chi(t)$ and a phase $2\psi(t)$ that are both fixed by the sidereal time; no free phase remains. For the illustrative latitude $\varphi = 52.5°$, $\sin^2\chi$ reaches its maximum value of 1 at LST ≈ 5.8 h and 16.6 h ($H \approx \mp 5.4$ h) and its minima of ≈0.74 at LST ≈ 11.2 h and ≈0.51 at LST ≈ 23.2 h. The orbital motion of the Earth (29.8 km/s) adds an annual modulation of V^2 of up to about ±16%.

Expected amplitude and re-analysis strategy. With the present bound $|\Delta\nu/\nu| \lesssim 10^{-18}$ [20], the amplitude is limited to $A_{ESMT} \lesssim 6.6\times10^{-13}$; cavities reaching 10^{-19}–10^{-20} would probe A_{ESMT} down to ≈10^{-14}–10^{-15}. Existing rotating-cavity datasets [19,20,64] can be re-analysed as follows: (i) take the published Fourier coefficients of the $2\omega_r$ modulation as functions of sidereal time; (ii) fit the one-parameter template above, with α_D, δ_D and the site latitude fixed, leaving only A_{ESMT} free; and (iii) compare its goodness of fit with that of the unconstrained Standard-Model-Extension fit [2]. A null result tightens the upper bound on A_{ESMT}, whereas a significant signal whose sidereal phase is inconsistent with the dipole direction rules out E8.

F2. Multi-Messenger Universal Dispersion Limit:

Mathematical Signal: Arrival time delay between gravitational wave (GW) and electromagnetic (EM) signals over distance D is $\Delta t = D|c_{GW}-c_{EM}|/c^2$.

Quantitative Bound: GW170817 establishes $|c_{GW}-c_{EM}|/c\lesssim 10^{-15}$ [24].

Falsification Condition: Detection of an energy-independent or distance-dependent velocity lag $\Delta t > 1$ ms over $D \geq 100$ Mpc in future binary neutron star mergers will refute Axiom E3.

F3. Subluminal Dispersion Sign and Magnitude:

Mathematical Signal: $\omega^2 = c^2k^2\left(1+\zeta_2 k^2 l^2\right)$ with $\zeta_2 < 0$ (subluminal dispersion). The time delay for high-energy photon E relative to low-energy photon is $\Delta t \approx \frac{3}{2}\frac{D}{c}\left(\frac{E}{E_{Pl}}\right)^2\left(\frac{l}{l_{Pl}}\right)^2$.

Quantitative Sensitivity: Fermi-LAT data [62, 63] constrain $l \lesssim l_{Pl} \approx 1.6\times10^{-35}$ m.

Falsification Condition: Observation of superluminal dispersion ($\zeta_2 > 0$ or $\zeta_1 \neq 0$) in TeV gamma-ray bursts will falsify the parity-symmetric medium model (E7).

F4. Black-Hole Ringdown Frequency Shift:

Mathematical Signal: Shift in quasi-normal mode (QNM) ringdown frequency $\Delta\omega_{QNM}/\omega_{QNM} \sim \epsilon\left(r_g/r_{horizon}\right)^2$ under modified inflow $v^2 = \frac{2GM}{r}\left(1+\epsilon\frac{r_g^2}{r^2}\right)$ (Eq. 24).

Sensitivity & Falsification: Next-generation detectors (LISA, Einstein Telescope) reaching 0.1% QNM spectroscopy precision will constrain $|\epsilon| \leq 10^{-3}$. Any statistically significant departure $|\epsilon| > 10^{-3}$ rules out the standard flow equation E4. Ringdown consistency tests of GR have already been carried out for GW150914 [65,66] and provide the analysis framework for this test.

8 Discussion

8.1 Novelty and degree of contribution

For transparency we classify the content of the paper at three levels.

Known results, synthesised: the Painlevé–Gullstrand form and the river model [27–29]; equivalence of the MacCullagh aether with Maxwell's equations [10]; Madelung equivalence [35]; radiance conservation; the flow form of flat FLRW; constraints on Le Sage gravity [42]. All of these are standard and are cited accordingly.

New organisation: (a) the unification of all the above within a single ontology, a medium with velocity field **v** and rotational perturbation **ξ**, with gravitation and electromagnetism as two scales of its motion; (b) Theorem 3 as an organising principle, a single relation for all clock effects verified numerically against GPS (Figure 2); (c) Proposition 1, stating gravitomagnetism as the spin of the medium and connecting it directly to the central notion of the Spin Theory; (d) the systematic translation of each axiom of a heterodox theory into a testable framework (Table 2 and Table B1), a methodological case study.

New, falsifiable hypotheses: E8 with prediction F1 (Lorentz violation locked to the CMB dipole, with the template (23)); H1 (charge as a rotational defect); F3 (sign of dispersion from parity symmetry of the medium).

We acknowledge that the new contribution lies in interpretation and in testable hypotheses rather than in calculations that go beyond existing theory. This is a common feature of medium theories that are empirically equivalent to relativity, as Lorentz's theory illustrated: they become experimentally distinguishable only when assumptions beyond the standard theory, such as E7 and E8, are introduced.

8.2 Comparison with general relativity and Einstein–aether theory

Within the domain of E1, ESMT is a reading of GR in a particular foliation. It differs from pure GR in assigning physical reality to that foliation (the preferred frame) and to the velocity field **v**. In GR, **v** is a gauge-dependent shift vector; in ESMT it is the velocity of a substance. Whether this is testable mirrors the Lorentz–Einstein question: only if the dynamics of the medium carries additional structure (E7, E8).

Compared with Einstein–aether theory [7], ESMT adds no dynamical field to the action; the preferred frame is fixed by a cosmological condition (E8). Minimal ESMT therefore evades the GW170817 constraint [8] naturally, but its preferred frame also has no dynamics of its own at low order.

8.3 Limitations and open problems

Existence of flat Euclidean slices. The Kerr spacetime admits no axisymmetric, conformally flat slicing that reduces smoothly to the Schwarzschild case [67]; Doran's form [30] has a twisted river structure, but its spatial slices are not exactly flat. E1 therefore holds exactly, with unit lapse, only in vacuum and marginally bound spherical symmetry and in flat cosmology, and to first post-Newtonian order in general; inside static matter with pressure a non-trivial lapse is required. Extending E1 to strong rotating fields is the main open problem.

Spin-2 Gravitational Waves and Elastic Shear Mechanics: A primary challenge for vector velocity medium models is accounting for transverse-traceless (spin-2) gravitational waves. In ESMT, this is addressed phenomenologically by modeling the medium as a viscoelastic continuum capable of supporting symmetric shear stress tensors $u_{ij} = \frac{1}{2}\left(\partial_i \xi_j + \partial_j \xi_i - \frac{2}{3}\delta_{ij}\nabla\cdot\boldsymbol{\xi}\right)$. This tensor sector is distinct from the purely rotational field of E5 (whose shear modulus vanishes) and is introduced here phenomenologically.

Derivation Sketch: Linearized shear perturbations h_{ij} propagating on the flow background obey the Navier–Cauchy elastic equation $\rho_m \ddot{h}_{ij} = \mu \nabla^2 h_{ij}$, where μ is the shear modulus. Imposing transverse-traceless gauge conditions ($\partial^i h_{ij} = 0, h^i_i = 0$) isolates two independent tensor polarization modes ($h_+, h_\times$) satisfying $\Box h_{ij} = 0$ with wave speed $c_{GW} = \sqrt{\mu/\rho_m}$. Universality (E3) then requires $\mu/\rho_m = c^2$, consistent with the GW170817 bound [24]; a constructive model of the coupling of these modes to matter, reproducing the quadrupole formula, is left for future work.

Weinberg–Witten Evasion: The Weinberg–Witten theorem [68] forbids massless spin-2 particles in theories with a Lorentz-covariant, conserved energy-momentum tensor. ESMT can in principle evade this theorem because Lorentz invariance is not a fundamental symmetry of the underlying medium (E1, E8), but an emergent low-energy symmetry (Theorem 1). Consequently, the stress-energy tensor of the medium does not transform covariantly under fundamental Lorentz boosts at high energies, allowing massless tensor shear modes to exist without mathematical contradiction..

Universality of the cone. In analogue models each type of excitation typically has its own speed [3]. E3 requires all speeds to agree to $10^{-15} - 10^{-18}$; explaining this fine-tuning from microstructure is a challenge shared by all emergent theories.

Origin of charge and the Standard Model. H1 and H2 remain qualitative; mass ratios, the fine-structure constant and the gauge group $SU(3)\times SU(2)\times U(1)$ have not been reproduced.

Quantisation condition. Following Wallstrom [57], (21) must be added as a postulate; ESMT does not yet derive it from medium dynamics.

Quantum gravity. ESMT proposes no mechanism for quantising the medium at scale l.

8.4 Implications for the source theory

The analysis shows that the core intuition of the Spin Theory (Euclidean space, absolute time, a medium with spin as the basis of all interactions, slowing of processes rather than contraction of time, lensing as refraction, inertia as reaction to the medium) can be retained in a consistent, data-compatible theory. The

price is abandoning three specific ideas: a medium at rest around massive bodies (replaced by inflow), gravity by absorption (replaced by flow), and instantaneous propagation (replaced by propagation at c relative to the medium). The methodological lesson is that a physical intuition can be correct while the laws derived from it are wrong, and only rigorous mathematics and quantitative confrontation can separate the two.

9 Prospective applications

Relativistic geodesy and positioning. Theorem 3 provides a unified and intuitive presentation of relativistic corrections in global navigation satellite systems [46] and in chronometric geodesy with optical clocks, where height differences are measured through clock-rate differences [41]. With clocks reaching 10^{-18} stability, height differences of 1 cm become measurable; the "speed relative to the medium" viewpoint aids the design and teaching of such systems.

Transformation optics and metamaterials. Light propagating in a flowing medium with an effective index underlies transformation optics [69,70]. Structures emulating the flow (9) enable "optical black holes" and laboratory gravitational lenses for wave control and sensing.

Analogue gravity. ESMT specifies the structure to be emulated: a fluid with inflow profile $\sqrt{2GM/r}$ and the vortical component (15). Bose–Einstein condensate experiments [23] could test an analogue of Proposition 1: polarised phonons (in fluids supporting transverse modes) should rotate with the vorticity of the background flow.

Tests of fundamental physics. Prediction F1 supplies a concrete data-analysis strategy for Lorentz-invariance experiments, and F4 for gravitational-wave ringdown analyses.

Education. The unified medium presentation helps students visualise relativistic effects before mastering differential geometry, and illustrates how a theory can be reconstructed from its critique.

Applications suggested by the source theory, such as gravitational shielding, extraction of energy from the spatial medium or intervention in black-hole evolution, are not supported by ESMT; they conflict with constraint (2) and with energy conservation in E4.

10 Conclusions

We have constructed the Extended Spin-Medium Theory (ESMT) as a constrained reconstruction of the Spin Theory. Built upon eight axioms, ESMT quantitatively reproduces standard relativistic predictions—including clock-rate shifts (GPS, Pound–Rebka, muons), gravitational optics ($1.7512''$ solar deflection, Shapiro delay), planetary precession ($42.98''$/century for Mercury), gravitomagnetism (Gravity Probe B, LAGEOS), the equivalence principle, Maxwell's equations, and flat cosmology—as mathematical equivalences to standard geometries. The concept of "spin" is rigorously formulated as local medium vorticity $\Omega = \frac{1}{2}\nabla \times \mathbf{v}$, matching Lense–Thirring precession. Empirically refuted components of the source theory (Le Sage gravity, instantaneous propagation, velocity-relation law, centered cosmology) are discarded on quantitative grounds. ESMT remains empirically equivalent to standard physics in existing tests while offering four distinct, falsifiable predictions tied to the medium's preferred frame and microstructure. Major open challenges include constructing tensor dynamics for gravitational waves and extending flat slicing to strong rotating fields.

Funding: This research received no external funding.

Data availability statement: The data that support the findings of this study are available from the

corresponding authors upon reasonable request.

Declaration of competing interest: The authors declare that they have no known competing financial interests or personal relationships that could have appeared to influence the work reported in this paper.

Appendix A. Claims of the source theory excluded by data

Table A1. Claims of the source theory excluded by precision data

No.	Claim of the source theory	Decisive test	Outcome
1	Lorentz factor is a constant $(1/\sqrt{2})$	Stored muons; ion clocks [40,41]	Continuous $\gamma(v)$ measured
2	Clocks at equal geocentric distance run at equal rates	GPS operations [46]	+38.6 μs/day offset
3	Gyroscope axis is an absolute straight line	Gravity Probe B [45]	Geodetic and frame-dragging drift
4	Images are formed instantaneously	Lunar laser ranging [44]	≈2.5 s round trip
5	Light vanishes everywhere when the source stops	Cavity ring-down [43]	Persists for ~10 μs
6	Gravity from absorption of an isotropic flux	Shielding bound [42]; energy and drag (2)	Excluded by $>10^{19}$
7	Direct current flows only at the conductor surface	$R=\rho L/A$ scaling	Bulk conduction
8	Shell capacities 2q,4q,8q	Atomic spectra, periodic table	Capacities $2n^2$
9	Temperature scale $T\in[0,1]$	Planck spectrum	Kelvin scale
10	Cosmological redshift without expansion	SN Ia time dilation [47]; FIRAS [48]	$(1+z)$ dilation; blackbody CMB
11	Spherical universe with a centre	CMB isotropy; vorticity [49]	No centre; $(\omega/H)_0<4.7\times10^{-11}$

Appendix B. Dictionary: Spin Theory and ESMT

Table B1. Dictionary between the Spin Theory and ESMT

Spin Theory [9]	ESMT	Equation
Space photons at rest, spin $W=C$	Medium element; propagation at c relative to it	(4)
Spin $\omega=v/R$	Local angular velocity $\frac{1}{2}\nabla\times\mathbf{v}$	(3)
Scalar / directed spin	Irrotational inflow / solenoidal component	(7)
Mass spin m, medium pressure	Inflow $\sqrt{2GM/r}$	(5), (9)
Processes slowed by motion	Rate set by speed relative to medium	(11)
Right-triangle velocity law, hypotenuse c	Light clock; $w^2=u^2+v^2$ on circular orbits	(8), (13)
Straight line = gyroscope axis	Gyroscope axis fixed relative to medium element	Prop. 1, (16)
Lensing as refraction	Propagation on achromatic optical metric	(4), [56]
Magnetic spin, electric spin	Elastic rotation angle \$/2\$; rotational defects (H1)	(17)–(19)
Particles and antiparticles from opposite spin pairs	Topological solitons and anti-solitons (H2)	Sect. 5.6
Radiation temperature independent of distance	Brightness-temperature conservation	Thm. 4

Spin Theory [9]	ESMT	Equation
Absolute black point	Horizon where the inflow reaches c	(9), $r=2GM/c^2$
Absolute reference frame	Cosmic rest frame of the medium = CMB frame	E8

Appendix C. Detailed proofs

C.1 Theorem 1

Consider fields $\{\phi_a\}$ obeying linear or nonlinear hyperbolic equations of the form $g^{\mu\nu}\partial_\mu\partial_\nu\phi_a+F_a(\phi,\partial\phi)=0$, where $g^{\mu\nu}$ is the inverse of (4) with constant $\mathbf{v}$ and the F_a are Lorentz-scalar functions of the fields and their first derivatives (universality condition). The change of variables $\mathbf{x}'=\mathbf{x}-\mathbf{v}t$, $t'=t$ gives $g'^{\mu\nu}=\eta^{\mu\nu}$. For every Lorentz transformation Λ of η, if $\phi_a(x')$ is a solution then so is $\phi_a(\Lambda^{-1}x')$ (with the appropriate representation). A rod is a localised static solution; a clock is a localised periodic solution. Their images under Λ are a rod and a clock moving at the corresponding velocity; dimensionless quantities (the number of clock periods during the light transit time across the rod) are invariant. Hence every local experiment yields the same result irrespective of $\mathbf{v}$. ▫

C.2 Free-fall geodesic in the flow metric

For the metric (9), the timelike Killing vector ∂_t yields the conserved quantity $\mathcal{E}=-g_{t\mu}\dot{x}^\mu/c^2=(1-v^2/c^2)t-(v/c^2)r$ with $v=\sqrt{2GM/r}$, where the dot denotes $d/d\tau$. Substituting $r=-vt$ (co-moving inward drift) and $t=1$ gives $\mathcal{E}=1-v^2/c^2+v^2/c^2=1$, the specific energy of a particle at rest at infinity. The normalisation $g_{\mu\nu}\dot{x}^\mu\dot{x}^\nu=-c^2$ is satisfied since $d\mathbf{x}-\mathbf{v}dt=0$. The radial equation $\ddot{r}=-GM/r^2$ (in τ) holds because $\frac{d}{d\tau}\left(-\sqrt{2GM/r}\right)=\frac{GM}{r^2}\frac{r}{v}=-\frac{GM}{r^2}$. ▫

C.3 Relation (16)

With $\mathbf{v}=(2G/c^2)\mathcal{J}\times\mathbf{r}/r^3$, apply the dipole identity $\nabla\times(\mathbf{m}\times\mathbf{r}/r^3)=[3(\mathbf{m}\cdot\hat{\mathbf{r}})\hat{\mathbf{r}}-\mathbf{m}]/r^3$ for $r\neq0$, and multiply by $\frac{1}{2}$. ▫

C.4 Relation (22)

From $\mathbf{r}=a(t)\mathbf{x}$: $d\mathbf{r}=a\,d\mathbf{x}+\dot{a}\mathbf{x}\,dt$, so $a\,d\mathbf{x}=d\mathbf{r}-H\mathbf{r}\,dt$ and $a^2d\mathbf{x}^2=|d\mathbf{r}-H\mathbf{r}\,dt|^2$. ▫

Appendix D. Numerical code

The following Python code (NumPy, SciPy) reproduces the numbers in Table 3 and Figure 2.

```
import numpy as np
from scipy.integrate import solve_ivp
from scipy.optimize import brentq
c = 299792458.0
# --- GPS, Theorem 3 (with J2) ---
GM = 3.986004418e14; RE = 6.3781e6; a = 2.656175e7; J2 = 1.08263e-3
vE = 7.2921e-5 * RE
ground = (GM/RE*(1 + J2/2) + vE**2/2) / c**2  # w^2/(2c^2), ground
sat    = 1.5*GM/(a*c**2)                      # (u^2+2GM/r)/(2c^2), u^2=GM/a
print("GPS us/day:", (ground - sat)*86400e6)   # -> 38.576
# --- Light deflection: u'' + u = 3 m u^2 ---
```

```
GMs = 1.32712440018e20; Rs = 6.957e8; m = GMs/c**2
f = lambda p, y: [y[1], -y[0] + 3*m*y[0]**2]
ev = lambda p, y: y[0]; ev.terminal = True
s = solve_ivp(f, [0, np.pi], [1/Rs, 0], rtol=1e-12, atol=1e-20, events=ev)
print("deflection arcsec:", (2*s.t_events[0][0] - np.pi)*206264.806)  # 1.7512
# --- Mercury: u'' + u = GM/h^2 + 3 m u^2, h^2 = GM p ---
A = 5.7909e10; e = 0.205630; P = 87.969*86400; p = A*(1 - e**2)
g = lambda q, y: [y[1], -y[0] + 1/p + 3*m*y[0]**2]
s = solve_ivp(g, [0, 2.5*np.pi], [1/(A*(1 - e)), 0], rtol=1e-13,
        atol=1e-22, dense_output=True, max_step=1e-3)
q2 = brentq(lambda q: s.sol(q)[1], 2*np.pi - 0.01, 2*np.pi + 0.01)
print("perihelion arcsec/century:",
    (q2 - 2*np.pi)*206264.806*36525*86400/P)  # -> 42.98
# --- Shapiro round trip, Earth-Saturn (r2 = 9.2 AU), b = 1.6 R_sun ---
AU = 1.495978707e11
print("Shapiro us:", 4*GMs/c**3*np.log(4*AU*9.2*AU/(1.6*Rs)**2)*1e6)  # ~264
# --- Le Sage constraints, Eqs. (1)-(2) ---
G = 6.67430e-11; Me = 5.972e24; kap = 1e-22
Is = G*c/kap**2
print("P/Lsun:", 4*np.pi*Is*kap*Me/3.828e26,
    "drag:", 4*np.pi*Is*kap*3e4/c**2)
```

Funding: The authors declare that no funds, grants, or other support were received during the preparation of this manuscript.

Data Availability Statement: The data that support the findings of this study are available from the corresponding authors upon reasonable request.

Declaration of competing interest: The authors declare that they have no known competing financial interest or personal relationships that could have appeared to influence the work reported in this paper.

References

[1] C.M. Will (2014). The confrontation between general relativity and experiment. Living Rev. Relativ., 17, 4. https://doi.org/10.12942/lrr-2014-4

[2] V.A. Kostelecký, N. Russell (2011). Data tables for Lorentz and CPT violation. Rev. Mod. Phys., 83, 11–31. https://doi.org/10.1103/RevModPhys.83.11

[3] C. Barceló, S. Liberati, M. Visser (2011). Analogue gravity. Living Rev. Relativ., 14, 3. https://doi.org/10.1007/s41114-026-00064-9

[4] G.E. Volovik (2003). The Universe in a Helium Droplet. Oxford University Press, Oxford.

[5] A.D. Sakharov (1991). Vacuum quantum fluctuations in curved space and the theory of gravitation. Sov. Phys. Usp., 34, 394. https://doi.org/10.1070/PU1991v034n05ABEH002498

[6] T. Jacobson (1995). Thermodynamics of spacetime: the Einstein equation of state. Phys. Rev. Lett., 75, 1260–1263. https://doi.org/10.1103/PhysRevLett.75.1260

[7] T. Jacobson, D. Mattingly (2001). Gravity with a dynamical preferred frame. Phys. Rev. D, 64, 024028. https://doi.org/10.1103/PhysRevD.64.024028

[8] J. Oost, S. Mukohyama, A. Wang (2018). Constraints on Einstein-aether theory after GW170817. Phys. Rev. D, 97, 124023. https://doi.org/10.1103/PhysRevD.97.124023

[9] T.T. Triet, T.T. Tien (2021). SPIN THEORY FOR THE UNIVERSE. Eliva Press, 105. ISBN: 978-1636484624

[10] J. MacCullagh (1848; read 1839). An essay towards a dynamical theory of crystalline reflexion and refraction. Trans. R. Ir. Acad., 21, 17–50. [suspicious link removed]

[11] J.C. Maxwell (1861, 1862). On physical lines of force. Philos. Mag., 21, 161–175, 281–291, 338–348; 23, 12–24, 85–95.

https://www.math.ucdavis.edu/~temple/MAT22C/MaxwellOnPhysicalLinesOfForce.pdf

[12] W. Thomson (Lord Kelvin) (1867). On vortex atoms. Philos. Mag., 34, 15–24.

https://zapatopi.net/kelvin/papers/on_vortex_atoms.html

[13] H.A. Lorentz (1904). Electromagnetic phenomena in a system moving with any velocity smaller than that of light. Proc. K. Ned. Akad. Wet., 6, 809–831. https://doi.org/10.1007/978-94-015-3445-1_5

[14] A.A. Michelson, E.W. Morley (1887). On the relative motion of the Earth and the luminiferous ether. Am. J. Sci., 34, 333–345. https://doi.org/10.2475/ajs.s3-34.203.333

[15] A. Einstein (1905). Zur Elektrodynamik bewegter Körper. Ann. Phys., 322, 891–921. https://doi.org/10.1002/andp.19053221004

[16] J.S. Bell (1987). How to teach special relativity. In: Speakable and Unspeakable in Quantum Mechanics, pp. 67–80. Cambridge University Press, Cambridge.

https://doi.org/10.1017/CBO9780511815676.011

[17] H.R. Brown (2005). Physical Relativity: Space-time Structure from a Dynamical Perspective. Oxford University Press, Oxford. https://doi.org/10.1093/0199275831.001.0001

[18] R. Mansouri, R.U. Sexl (1977). A test theory of special relativity. I. Simultaneity and clock synchronization. Gen. Relativ. Gravit., 8, 497–513. https://doi.org/10.1007/BF00762634

[19] S. Herrmann, et al. (2009). Rotating optical cavity experiment testing Lorentz invariance at the level. Phys. Rev. D, 80, 105011. https://doi.org/10.1103/PhysRevD.80.105011

[20] M. Nagel, et al. (2015). Direct terrestrial test of Lorentz symmetry in electrodynamics to . Nat. Commun., 6, 8174. https://doi.org/10.1038/ncomms9174

[21] W.G. Unruh (1981). Experimental black-hole evaporation? Phys. Rev. Lett., 46, 1351–1353. https://doi.org/10.1103/PhysRevLett.46.1351

[22] M. Visser (1998). Acoustic black holes: horizons, ergospheres and Hawking radiation. Class. Quantum Grav., 15, 1767–1791. https://doi.org/10.1088/0264-9381/15/6/024

[23] J.R. Muñoz de Nova, K. Golubkov, V.I. Kolobov, J. Steinhauer (2019). Observation of thermal Hawking radiation and its temperature in an analogue black hole. Nature, 569, 688–691. https://doi.org/10.1038/s41586-019-1241-0

[24] B.P. Abbott, et al. (2017). Gravitational waves and gamma-rays from a binary neutron star merger: GW170817 and GRB 170817A. Astrophys. J. Lett., 848, L13. https://doi.org/10.3847/2041-8213/aa920c

[25] J.G. Williams, S.G. Turyshev, D.H. Boggs (2004). Progress in lunar laser ranging tests of relativistic gravity. Phys. Rev. Lett., 93, 261101. https://doi.org/10.1103/PhysRevLett.93.261101

[26] L. Shao, R.N. Caballero, M. Kramer, N. Wex, D.J. Champion, A. Jessner (2013). A new limit on local Lorentz invariance violation of gravity from solitary pulsars. Class. Quantum Grav., 30, 165019. https://doi.org/10.1088/0264-9381/30/16/165019

[27] P. Painlevé (1921). In 1921, a breaking-through solution, in general relativity. https://astromontgeron.fr/Painleve-article-english.pdf

[28] A. Gullstrand (1922). Allgemeine Lösung des statischen Einkörperproblems in der Einsteinschen Gravitationstheorie. Ark. Mat. Astron. Fys., 16(8), 1–15. https://inspirehep.net/literature/1235877

[29] A.J.S. Hamilton, J.P. Lisle (2008). The river model of black holes. Am. J. Phys., 76, 519–532.

https://doi.org/10.1119/1.2830526

[30] C. Doran (2000). New form of the Kerr solution. Phys. Rev. D, 61, 067503.

https://doi.org/10.1103/PhysRevD.61.067503

[31] T.H.R. Skyrme (1961). A non-linear field theory. Proc. R. Soc. Lond. A, 260, 127–138. https://doi.org/10.1098/rspa.1961.0018

[32] E. Witten (1983). Current algebra, baryons, and quark confinement. Nucl. Phys. B, 223, 433–444. https://doi.org/10.1016/0550-3213(83)90064-0

[33] D. Finkelstein, J. Rubinstein (1968). Connection between spin, statistics, and kinks. J. Math. Phys., 9, 1762–1779. https://doi.org/10.1063/1.1664510

[34] L. Faddeev, A.J. Niemi (1997). Stable knot-like structures in classical field theory. Nature, 387, 58–61. https://doi.org/10.1038/387058a0

[35] E. Madelung (1927). Quantentheorie in hydrodynamischer Form. Z. Phys., 40, 322–326. https://doi.org/10.1007/BF01400372

[36] R.P. Feynman (1955). Application of quantum mechanics to liquid helium. Prog. Low Temp. Phys., 1, 17–53. https://doi.org/10.1016/S0079-6417(08)60077-3

[37] Y. Couder, E. Fort (2006). Single-particle diffraction and interference at a macroscopic scale. Phys. Rev. Lett., 97, 154101. https://doi.org/10.1103/PhysRevLett.97.154101

[38] H. Kleinert (2008). Multivalued Fields in Condensed Matter, Electromagnetism, and Gravitation. World Scientific, Singapore.

https://hagenkleinert.de/documents/mvf/HagenKleinert_MultivaluedFields.pdf

[39] A Short History of Spin (2013). arXiv:1311.5016v1 [physics.hist-ph].

https://arxiv.org/html/1311.5016v1#S2

[40] J. Bailey, et al. (1977). Measurements of relativistic time dilatation for positive and negative muons in a circular orbit. Nature, 268, 301–305. https://doi.org/10.1038/268301a0

[41] C.W. Chou, D.B. Hume, T. Rosenband, D.J. Wineland (2010). Optical clocks and relativity. Science, 329, 1630–1633. https://doi.org/10.1126/science.1192720

[42] D.H. Eckhardt (1990). Gravitational shielding. Phys. Rev. D, 42, 2144–2145.

https://doi.org/10.1103/PhysRevD.42.2144

[43] A. O'Keefe, D.A.G. Deacon (1988). Cavity ring-down optical spectrometer for absorption measurements using pulsed laser sources. Rev. Sci. Instrum., 59, 2544–2551

https://doi.org/10.1063/1.1139895

[44] T.W. Murphy (2013). Lunar laser ranging: the millimeter challenge. Rep. Prog. Phys., 76, 076901. https://doi.org/10.1088/0034-4885/76/7/076901

[45] C.W.F. Everitt, et al. (2011). Gravity Probe B: final results of a space experiment to test general relativity. Phys. Rev. Lett., 106, 221101. https://doi.org/10.1103/PhysRevLett.106.221101

[46] N. Ashby (2003). Relativity in the Global Positioning System. Living Rev. Relativ., 6, 1. https://doi.org/10.12942/lrr-2003-1

[47] S. Blondin, et al. (2008). Time dilation in type Ia supernova spectra at high redshift. Astrophys. J., 682, 724–736. https://doi.org/10.1086/589568

[48] D.J. Fixsen, et al. (1996). The cosmic microwave background spectrum from the full COBE FIRAS data set. Astrophys. J., 473, 576–587. https://doi.org/10.1086/178173

[49] D. Saadeh, S.M. Feeney, A. Pontzen, H.V. Peiris, J.D. McEwen (2016). How isotropic is the Universe? Phys. Rev. Lett., 117, 131302. https://doi.org/10.1103/PhysRevLett.117.131302

[50] C.W. Misner, D.H. Sharp (1964). Relativistic equations for adiabatic, spherically symmetric gravitational collapse. Phys. Rev., 136, B571–B576. https://doi.org/10.1103/PhysRev.136.B571

[51] P. Touboul, et al. (2022). MICROSCOPE mission: final results of the test of the equivalence principle. Phys. Rev. Lett., 129, 121102. https://doi.org/10.1103/PhysRevLett.129.121102

[52] B. Bertotti, L. Iess, P. Tortora (2003). A test of general relativity using radio links with the Cassini spacecraft. Nature, 425, 374–376. https://doi.org/10.1038/nature01997

[53] I.I. Shapiro (1964). Fourth test of general relativity. Phys. Rev. Lett., 13, 789–791. https://doi.org/10.1103/PhysRevLett.13.789

[54] B. Mashhoon (2003). Gravitoelectromagnetism: a brief review. arXiv:gr-qc/0311030.

[55] I. Ciufolini, E.C. Pavlis (2004). A confirmation of the general relativistic prediction of the Lense–Thirring effect. Nature, 431, 958–960. https://doi.org/10.1038/nature03007

[56] W. Gordon (1923). Zur Lichtfortpflanzung nach der Relativitätstheorie. Ann. Phys., 377, 421–456. https://doi.org/10.1002/andp.19233772202

[57] T.C. Wallstrom (1994). Inequivalence between the Schrödinger equation and the Madelung hydrodynamic equations. Phys. Rev. A, 49, 1613–1617. https://doi.org/10.1103/PhysRevA.49.1613

[58] Planck Collaboration, N. Aghanim, et al. (2020). Planck 2018 results. VI. Cosmological parameters. Astron. Astrophys., 641, A6. https://doi.org/10.1051/0004-6361/201833910

[59] Planck Collaboration, N. Aghanim, et al. (2020). Planck 2018 results. I. Overview and the cosmological legacy of Planck. Astron. Astrophys., 641, A1. https://doi.org/10.1051/0004-6361/201833880

[60] R.V. Pound, G.A. Rebka (1960). Apparent weight of photons. Phys. Rev. Lett., 4, 337–341. https://doi.org/10.1103/PhysRevLett.4.337

[61] R.F.C. Vessot, et al. (1980). Test of relativistic gravitation with a space-borne hydrogen maser. Phys. Rev. Lett., 45, 2081–2084. https://doi.org/10.1103/PhysRevLett.45.2081

[62] A.A. Abdo, et al. (2009). A limit on the variation of the speed of light arising from quantum gravity effects. Nature, 462, 331–334. https://doi.org/10.1038/nature08574

[63] V. Vasileiou, et al. (2013). Constraints on Lorentz invariance violation from Fermi-Large Area Telescope observations of gamma-ray bursts. Phys. Rev. D, 87, 122001. https://doi.org/10.1103/PhysRevD.87.122001

[64] H. Müller, P.L. Stanwix, M.E. Tobar, E. Ivanov, P. Wolf, S. Herrmann, A. Senger, E. Kovalchuk, A. Peters (2007). Tests of relativity by complementary rotating Michelson–Morley experiments. Phys. Rev. Lett., 99, 050401. https://doi.org/10.1103/PhysRevLett.99.050401

[65] B.P. Abbott, et al. (LIGO Scientific and Virgo Collaborations) (2016). Observation of gravitational waves from a binary black hole merger. Phys. Rev. Lett., 116, 061102. https://doi.org/10.1103/PhysRevLett.116.061102

[66] B.P. Abbott, et al. (LIGO Scientific and Virgo Collaborations) (2016). Tests of general relativity with GW150914. Phys. Rev. Lett., 116, 221101. https://doi.org/10.1103/PhysRevLett.116.221101

[67] A. Garat, R.H. Price (2000). Nonexistence of conformally flat slices of the Kerr spacetime. Phys. Rev. D, 61, 124011. https://doi.org/10.1103/PhysRevD.61.124011

[68] S. Weinberg, E. Witten (1980). Limits on massless particles. Phys. Lett. B, 96, 59–62. https://doi.org/10.1016/0370-2693(80)90212-9

[69] U. Leonhardt, T.G. Philbin (2006). General relativity in electrical engineering. New J. Phys., 8, 247. https://doi.org/10.1088/1367-2630/8/10/247

[70] J.B. Pendry, D. Schurig, D.R. Smith (2006). Controlling electromagnetic fields. Science, 312, 1780–1782. https://doi.org/10.1126/science.1125907